



Modeling and simulation of the Vigor wave energy converter

*Master's Thesis in the Master Degree Programme,
Sustainable Energy Systems*

EGILL MARON THORBERGSSON

Department of Energy and Environment
CHALMERS UNIVERSITY OF TECHNOLOGY
Department of Physics
UNIVERSITY OF GOTHENBURG
Göteborg, Sweden 2009

MASTER'S THESIS 2009

Modeling and simulation of the Vigor wave energy
converter

Master's Thesis in Sustainable Energy Systems
EGILL MARON THORBERGSSON

Examiner: Magnus Karlsteen

Department of Energy and Environment
CHALMERS UNIVERSITY OF TECHNOLOGY
Department of Physics
UNIVERSITY OF GOTHENBURG

Göteborg, Sweden 2009

Modeling and simulation of the Vigor wave energy converter
EGILL MARON THORBERGSSON

© EGILL MARON THORBERGSSON, 2009

Master's Thesis 2009
Department of Energy and Environment
Chalmers University of Technology
Department of Physics
University of Gothenburg
SE-412 96 Göteborg
Sweden
Telephone: + 46 (0)31-772 1000

Cover:
Artist impression of the Vigor wave energy converter

Name of printers/ Department of Physics
Göteborg, Sweden 2009

Modeling and simulation of the Vigor wave energy converter
Master's Thesis in Sustainable Energy Systems
EGILL MARON THORBERGSSON
Department of Energy and Environment
Chalmers University of Technology
Department of Physics
University of Gothenburg

Abstract

The need to make renewable energy a larger part in today's electricity generation is increasing because of environmental issues and energy security. A potential resource of energy that is starting to attract more attention is the energy in ocean waves. There is no commercial approach available but a large number of applications are competing to be the first ones to enter the market. A new approach, which was invented by Daniel Ehrnberg, has showed good potential. The approach is still in the design phase and a number of problems are still unsolved. In this thesis two problems are tackled; the interaction of the device and the ocean, and how to calculate the power output of the device. The solution to the first problem shows how the device will react to ocean waves. The solution to the second problem gives an idea of the energy potential of the device. The potential energy output of the the device is calculated for four different locations; two in Iceland, one in Ireland and Sweden. The conclusion is that the device can reach high efficiency of converting the wave energy into useful energy but works only when the waves are optimal for the device.

Keywords: Energy. Renewable energy. Ocean wave energy. Wave energy converters. Ocean waves. Electricity generation technology.

Acknowledgements

Takk - Thanks - Tack!

Some words too express gratitude to those who have helped me along the way. Special thanks to my advisor and examiner of the project Magnus Karlsteen. He helped me overcome my concerns and problems with discussion and guidance. I want to thank Daniel Ehrnberg, the inventor of the new approach, for discussions about the working principles of the device. Thanks to Andreas Albertsson the project manager from GU holding for keeping the work going.

Special thanks to Srdjan Sasic professor in fluid dynamics at the applied dynamics department of Chalmers, for discussion about the models for fluid dynamics.

Thanks to Frida Holmquis, Oliver Salamon, Linn Svärd and Kristoffer Weywadt for providing me the wave data from Sweden and Ireland.

This master thesis project received a grant from the energy research fund of Landsvirkjun, an energy company located in Iceland.

Egill Maron Thorbergsson
June 23, 2009
Göteborg

Contents

1	Introduction	1
2	Wave theory	3
2.1	Mathematical model of waves	3
2.2	Energy in waves	8
2.3	Statistical analysis of waves	9
3	Wave energy converters	11
3.1	Description of Vigor wave energy converter	11
3.2	Other wave energy converter - Pelamis	12
4	Problem statements	13
4.1	Interaction between the hose and the ocean	13
4.2	Flow inside the hose	13
5	Models description	14
5.1	Interaction between the hose and the ocean	14
5.2	Flow inside the hose	16
6	Results	19
6.1	Interaction between the hose and the ocean	19
6.2	Flow inside the hose	21
7	Conclusion	26
7.1	Future research	26

1 Introduction

The electricity usage is growing all over the globe and predictions indicate that electricity generation will increase by 77 percent from the year 2006 to 2030 taking into account today's global economic recession [2]. Primary energy use has doubled every thirty years since the early 1880s. Developing countries are seeing large increase in electricity consumption, as can be seen in China where there are around 2 new coal power plants constructed each week [3]. Governments are starting to realize how dangerous climate change is, e.g. the European Union has the target to reduce green house gas emissions by 20 percent before the year 2020 compared to emissions in the year 1990. This means that there is a high pressure to increase renewable energy share in the electricity generation. The electricity scenery in the year 2006 was that 16% comes from hydro, 15% nuclear, 20% gas, 6% oil, 41% coal/pet and 2% is geothermal, solar wind, combustible renewable and waste, and heat, based on 18,930 TWh/yr [1].

The energy need of human kind is small compared to the energy in nature. The energy flux from the sun that reach Earth is estimated to be around 5,440,000 EJ/yr. The winds, waves and the ocean currents are estimated to be around 11,700 EJ/yr while in the year 2006 anthropogenic energy use was around 490 EJ/yr (136,000 TWh/yr) [3, 1].

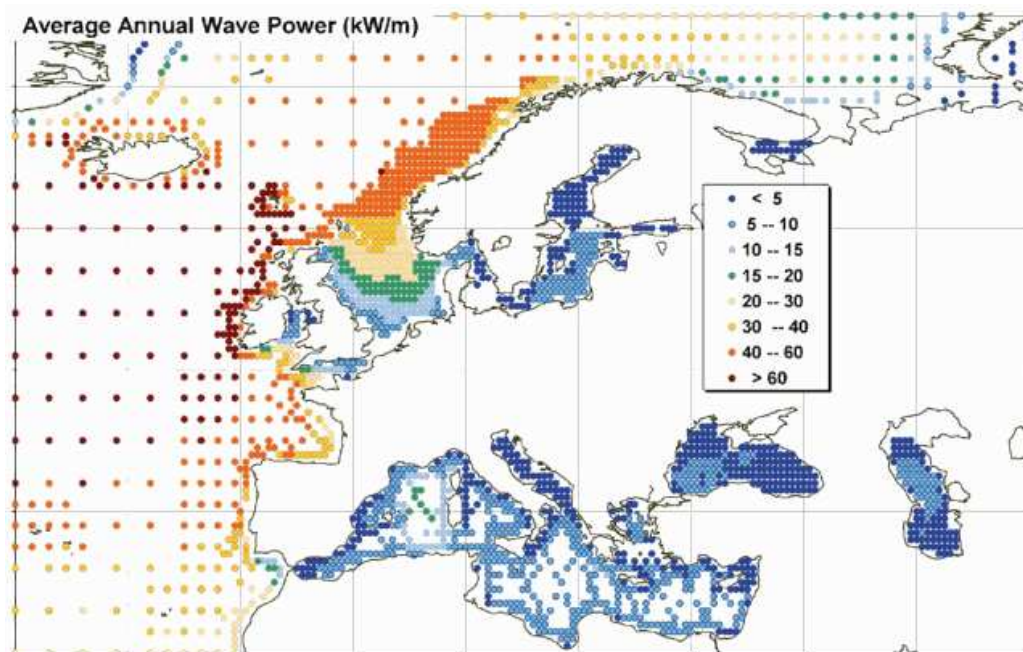


Figure 1.1: Annual mean wave power estimates (kW per meter of wave front) for European waters (data from the ECMWF WAM model archive; calibrated and corrected by Fugro OCEANOR against a global buoy and Topex satellite altimeter database) [5].

One resource of renewable energy that has not received much attention is the energy in ocean waves. The energy potential in ocean waves is quite high. Waves are a result from winds that blow over the oceans, and wind is a result from temperature difference across the Earth, which is formed from solar energy. The waves start by the random nature of pressure pulses, from wind, acting on the water surface and the subsequent, complex growth of the perturbations in the free surface. The wind then acts harder and harder on these perturbations

and form waves. The potential power in waves are estimated to be of the same magnitude as the average power consumption of humans, which is around 2 TW. The potential to utilise this is not very high and a conservative estimate of the utilization is around 10 to 25 percent [5]. This suggest though that wave power could make a significant contribution to the energy mix. For example on a typical day, about 1 TWh of wave energy enters the coastal waters of the British Isles. This corresponds to approximately the average daily electricity consumption in the UK. The estimated yearly average wave power in Europe is shown in figure 1.1 which shows the annual mean wave power estimates in kW per meter of wave front [5]. The wave power potential is very high along the coast of Portugal, Ireland, Iceland, Faroe Islands and Norway.

There are number of competing approaches trying to be the first to make the final leap towards commercial applications, and it is still unclear which one will be the winner.

One of the competing approaches was invented by Daniel Ehrnberg [7] which showed good economical and environmental aspects. More detailed analysis of the approach will be made in this thesis and a more detailed model for power calculations will be presented. This model will be used to calculate the energy potential at for four different locations, two in Iceland, one in Ireland and one in Sweden.

2 Wave theory

Before going into the mathematical theory of ocean waves, it is good to have some idea about the movement of real waves, and the flow of the sea. Start by imagine some small object floating in the ocean, e.g. a bottle (that hopefully somebody finds and recycles). The bottle will move forward during the crest, pause as the trough comes, and moves backwards in the trough, nearly to the original position. This motion is quite close to a circular path.

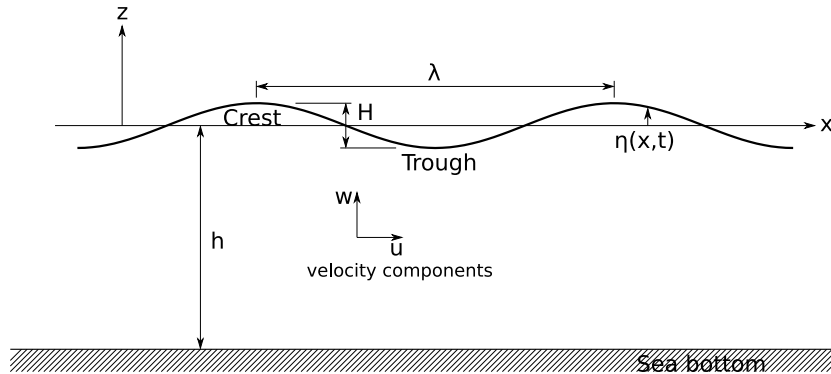


Figure 2.1: Wave characteristics and definition of variables.

A two dimensional plain wave is shown in figure 2.1, propagating in the x direction, with its characteristics. The difference between the surface elevation of the crest and the trough is defined as the wave height H , and the time required for the bottle to reach it original position is defined as the wave period T . The still water level defines the origin of z and the free water surface is defined as η . The distance from still water level to the bottom is defined as h . The distance between two adjacent crests is defined as the wave length λ . Wave lengths are always much larger than wave heights. When waves are too high they are much like a house of cards, unstable and have a tendency to fall apart at the slightest nudge [11].

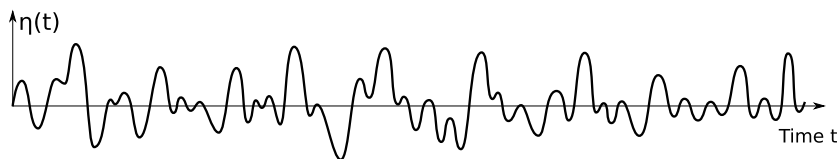


Figure 2.2: Surface elevation of a real waves as a function of time.

Real waves do not have the same look wave after wave and do not always propagate in the same direction. The surface elevation of a real waves would look similar as figure 2.2 shows over a time period.

2.1 Mathematical model of waves

The basic mathematical model of ocean waves was developed mainly by G.B. Airy and Laplace and is known as Airy's theory, small amplitude theory, linear wave theory and first-order theory. A detailed derivation of the theory can be found in e.g. [6] and [9]. The derivation for the mathematical model and the energy in waves has been adopted from Ref. [6] chapters 3 and 4.

Definition of variables

ϕ :	velocity potential for the flow
ψ :	stream function
\mathbf{u} :	velocity vector for the flow
ρ :	density for sea
ν :	viscosity for sea
σ :	the angular frequency of the wave
k :	the wave number
C_w :	the wave velocity or celerity $C_w = \lambda/T$
C_g :	the group wave velocity or group celerity
t :	time
p :	pressure

The linear wave theory is based on two fundamental equations and some simple boundary conditions. When these equations and boundary conditions are linearised, freely propagating harmonic waves are solutions to the equations. The governing differential equations are hydrodynamic equations which express conservation of mass and momentum, the continuity equation

$$\frac{\partial \rho}{\partial t} + \nabla \cdot (\rho \mathbf{u}) = 0 \quad (2.1)$$

and the Navier-Stokes equation

$$\frac{D\mathbf{u}}{Dt} \equiv \frac{\partial \mathbf{u}}{\partial t} + (\mathbf{u} \cdot \nabla)\mathbf{u} = -\frac{1}{\rho}\nabla p_{tot} + \nu\nabla^2\mathbf{u} + \mathbf{g}. \quad (2.2)$$

The assumptions that are used to find a solution to the differential equations are

- The amplitude, $H/2$, of the surface disturbance is very small compared to the wave length λ and the water depth h . This is the main assumption in linear wave theory.
- The velocity head $(u^2 + w^2)/(2g)$ is small compared with the hydrostatic pressure head $\rho g z$. The vertical and horizontal water particle velocities are w and u , respectively.
- The water depth h is uniform.
- The water is inviscid, $\nu = 0$, and irrotational, $\nabla^2\psi = 0$. This is reasonable because the turbulence from bottom does not penetrate very far into the main body.
- The water is incompressible $\frac{D\rho}{Dt} = 0$ and homogeneous, which excludes acoustic and internal wave phenomena.
- The Coriolis forces due to earth's rotation are negligible, the wave lengths need to be shorter than a few kilometres.
- Surface tension is negligible, wave lengths need to be longer than a few centimetres.
- The sea floor is smooth and impermeable.
- The sea level atmospheric pressure p_a is uniform.

The boundary conditions to find a solution to equations 2.1 and 2.2 are of the kinematic nature, related to the motions of the water particles and the dynamic nature, related to forces acting on the water particles.

The bottom boundary condition is defined as that the flow at the bottom is tangent to the bottom and that the particles will not penetrate the bottom. There are two boundary conditions at the free surface, kinematic and dynamic. The kinematic states that there is no flow across the interface, i.e. particles do not leave the surface. The dynamic free surface boundary conditions states that the pressure on the free surface is uniform along the wave form. The lateral boundary conditions is controlled by the assumption that the wave is periodic.

The velocity potential that describes a progressive wave is found using all the assumptions above, appropriate boundary conditions and that the waves have a small steepness, $|\nabla\eta| \ll 1$, and the non-linear terms are neglected. One of the analytical solutions is then the velocity potential

$$\phi = -\frac{H}{2} \frac{g}{\sigma} \frac{\cosh(k(h+z))}{\cosh(kh)} \sin(kx - \sigma t). \quad (2.3)$$

Using the periodic boundary conditions the angular frequency and wave number can be found

$$\sigma = \frac{2\pi}{T} \quad (2.4)$$

$$k = \frac{2\pi}{\lambda}. \quad (2.5)$$

The water surface elevation can then be found using the velocity potential (eq 2.3),

$$\eta(x, t) = \frac{1}{g} \left[\frac{\partial\phi}{\partial t} \right]_{z=0} = \frac{H}{2} \cos(kx - \sigma t). \quad (2.6)$$

Having the velocity potential it is easy to find the horizontal (u) and vertical (w) velocity components

$$u = -\frac{\partial\phi}{\partial x} = \frac{H}{2} \sigma \frac{\cosh(k(h+z))}{\sinh(kh)} \cos(kx - \sigma t) \quad (2.7)$$

$$w = -\frac{\partial\phi}{\partial z} = \frac{H}{2} \sigma \frac{\sinh(k(h+z))}{\sinh(kh)} \sin(kx - \sigma t). \quad (2.8)$$

Using the dynamic boundary conditions that there is zero pressure at the surface the relationship between angular frequency (σ) and wave number (k) can be found

$$\sigma^2 = gk \tanh(kh). \quad (2.9)$$

The relationship in equation 2.9 is often called the dispersion equation because it describes how a field of propagating waves, consisting of many frequencies, would separate or “disperse” due to the different wave speeds of each wave [6].

An important factor is the group velocity. Waves in the ocean do not all have the same frequencies. If two harmonic waves, that have slightly different frequencies, are added together then they will reinforce each other when they are in phase, when the crests of the waves coincide. They will cancel each other at another moment, as shown in figure 2.3. The group has a maximum height, where the two waves are in phase. The velocity of that point is, by definition the group velocity, the phase speed of the surface elevations envelope [10]. The group velocity, when the difference between the frequencies is infinite small, is

$$C_g = \frac{\partial\sigma}{\partial k} = \frac{1}{2} \left(1 + \frac{2kh}{\sinh(2kh)} \right) C_w. \quad (2.10)$$

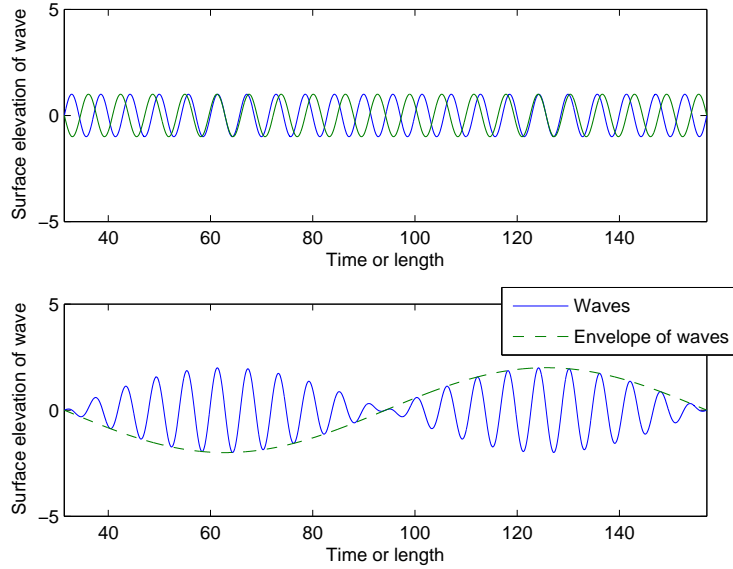


Figure 2.3: The above figure shows two waves with slightly different frequencies. Figure below shows the waves added together and shows how a group of waves is formed.

2.1.1 Simplifications for shallow and deep water

The hyperbolic functions have convenient asymptotes for shallow and deep water, shown in figure 2.4. The limits used here are

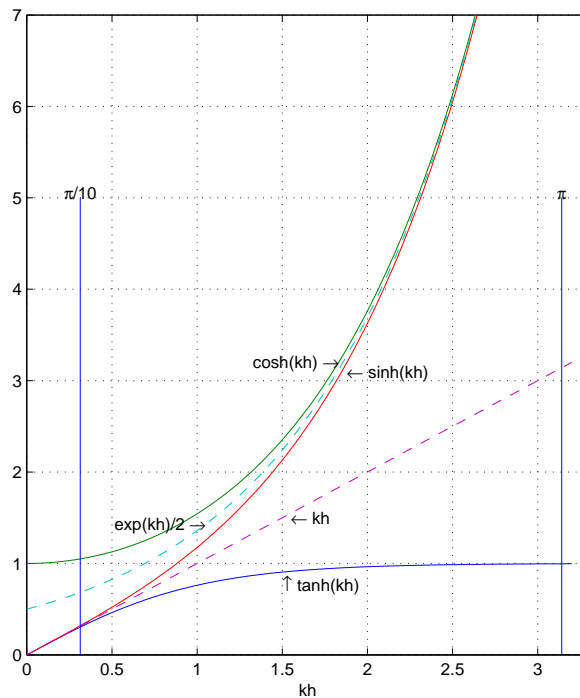


Figure 2.4: Asymptotes to hyperbolic functions. Shallow water is $kh < \pi/10$ and deep water is $kh > \pi$ water.

$$\begin{array}{ll}
\text{shallow water:} & kh < \frac{\pi}{10}, \\
\text{intermediate depth:} & \frac{\pi}{10} < kh < \pi, \\
\text{deep water:} & \pi < kh.
\end{array}$$

It is helpful to use these asymptotes to obtain simplified forms of the equations describing wave motion. For more detailed derivations one can look at e.g. ref. [6]. The equations when reduced for shallow and deep water approximations are shown in table 2.1

Table 2.1: Approximations for equations in shallow ($kh < \pi/10$) and deep ($kh > \pi$) water

Shallow water	Deep water
$\sigma = \sqrt{gk^2h}$	$\sigma = \sqrt{gk}$
$\lambda = \sqrt{gh}T$	$\lambda = \frac{gT^2}{2\pi}$
$C_w = \sqrt{gh}$	$C_w = \frac{gT}{2\pi}$
$C_g = C_w$	$C_g = \frac{1}{2}C_w$
$u = \frac{H}{2}\sigma\frac{1}{kh}\cos(kx - \sigma t)$	$u = \frac{H}{2}\sigma\exp(kz)\cos(kx - \sigma t)$
$w = \frac{H}{2}\sigma\left(1 + \frac{1}{z}\right)\sin(kx - \sigma t)$	$w = \frac{H}{2}\sigma\exp(kz)\sin(kx - \sigma t).$

2.2 Energy in waves

The total energy in waves is the sum of potential and kinetic energy of the particles in the ocean. The potential is from the displacement of the free surface, i.e. particles are moved from rest to some other position, and the kinetic energy, is due to the fact that the particles in the ocean are moving [6, 10]. The potential energy of the wave-induced potential in the entire water, from bottom to surface is equal to the potential energy in the presence of wave minus the potential energy in the absence of the wave. The potential energy averaged over one period per unit surface area is then

$$\overline{E}_{potential} = \overline{\int_{-h}^{\eta} \rho g z dz} - \overline{\int_{-h}^0 \rho g z dz} = \overline{\int_0^{\eta} \rho g z dz} = \frac{\rho g H^2}{16} \quad (2.11)$$

where the over-bar represents time-averaging.

The kinetic energy time-averaged over one time period per unit surface area is

$$\overline{E}_{kinetic} = \overline{\int_{-h}^{\eta} \frac{1}{2} \rho g (u + w)^2 dz} = \frac{\rho g H^2}{16} \quad (2.12)$$

using equations 2.7 and 2.8 for horizontal and vertical velocities of the particles respectively. The total time-averaged wave-induced energy density $\overline{E} = \overline{E}_{potential} + \overline{E}_{kinetic}$ per surface area, using the approximations of the linear wave theory is

$$\overline{E} = \frac{1}{8} \rho g H^2. \quad (2.13)$$

The total average energy per wave per unit width is then

$$\overline{E}_{\lambda} = \frac{1}{8} \rho g H^2 \lambda. \quad (2.14)$$

2.2.1 Energy transport

As the small-amplitude waves travel across the ocean they do not transmit mass as they propagate, because the trajectories of the water particles are closed. They do however carry their potential and kinetic energy with them. The wave energy is transported only by the work done by the wave induced pressure when using the linear approximations [10]. The energy transport, P , in waves per wave and per unit length wave-front is

$$P \approx \overline{\int_{-h}^0 p_{wave} u dz} = \left(\frac{1}{8} \rho g H^2 \right) \frac{1}{2} \left(1 + \frac{2kh}{\sinh(2kh)} \right) \frac{\sigma}{k} \quad (2.15)$$

where the wave induced pressure is [10]

$$p_{wave} = \frac{1}{2} \rho g H \frac{\cosh(k(h+z))}{\cosh(kh)} \sin(\sigma t - kx) \quad (2.16)$$

It is only necessary to integrate up to the mean free surface to retain the terms to the second order in wave height. The energy transport per wave per unit width can be expressed in a more useful form

$$P = EC_g \quad (2.17)$$

The equations for the energy transport can be simplified for shallow and deep water. For shallow water the energy transport is

$$P = \frac{\rho g^{3/2}}{8} H^2 \sqrt{h} \quad (2.18)$$

For deep water the energy transport is

$$P = \frac{\rho g^2}{32\pi} H^2 T \quad (2.19)$$

2.3 Statistical analysis of waves

Real waves are not monochromatic i.e. each wave has a different frequency. Today large number of companies and national agencies collect wave data all around the globe. Characterising the waves in the wave record is based on averaging all of the individual wave heights and periods in the record. The most common way to describe wave height is with what is called the significant wave height H_s or also called the mean of the highest one-third of waves

$$H_s = H_{1/3} = \frac{1}{N_{waves}/3} \sum_{j=1}^{N_{waves}/3} H_j \quad (2.20)$$

where j is not the sequence number in the record but the rank number of the wave ($j = 1$ is the highest, $j = 2$ is the second highest, etc) and where N_{waves} is the number of waves in the wave record. Experiments have shown that the value of this wave height is close to the height of random waves that would be reported by an observer [10]. The most common parameter for the wave period in random sea is T_z the zero crossing period, defined as the average period between successive up-crossing of the zero or the mean water level. The principals of wave height-distribution theory are less debated by experts in the field than on wave-period distribution. It is emphasized that the average period as defined here does not correspond to the period of the average wave height.

Surface wave heights H follow the Rayleigh probability density function $p(H)$ [6, 10]

$$p(H) = \frac{2H}{H_{rms}^2} \exp(-H^2/H_{rms}^2), \quad (2.21)$$

where the root mean square value of wave height is

$$H_{rms} = \sqrt{\frac{1}{N} \sum_{i=1}^{N_{waves}} H_i^2} \quad (2.22)$$

where i is the sequence number in the wave record data.

If the waves are not too steep and not in a shallow water, there is a (theoretically based) constant ratio between the various characteristics wave heights. The ratio between the root mean square value of wave height and the significant wave height is

$$H_{rms} = \frac{1}{\sqrt{2}} H_s \quad (2.23)$$

and the ration between the mean wave height (\bar{H}) and the significant wave height is

$$\bar{H} = \frac{\sqrt{\pi}}{2\sqrt{2}} H_s. \quad (2.24)$$

2.3.1 Wave data

Wave data from four different locations, shown in figure 2.5 are used to calculate the potential energy output from the Vigor. The exact locations for the buoys are shown in table 2.2 and the distance to shore. The depth at all locations is over 30 meters, and therefore all locations can be assumed to be deep water, and approximations for deep water will therefore be used for all locations.

The wave record is one data point for each hour. The buoys records the wave heights for 17.5 minutes and then takes average. This is then averaged for each hour. The wave record for Iceland is root mean square value, while for Ireland and Sweden it is significant wave height. The wave period in the wave data is the average zero crossing wave period. Using the wave



Figure 2.5: Position of buoys.

Table 2.2: Details of wave data. Locations of buoys and time span the buoys have recorded waves.

Location	Latitude	Longitude	Start [YYYYMMDD]	End [YYYYMMDD]	Distance to land [km]
Iceland B.	63°30'62" N	20°08'60" W	20031118	20090506	2.6
Iceland H.	64°11'81" N	15°11'31" W	20020101	20090506	7
Ireland	51°21'66" N	10°55'00" W	20050101	20090319	60
Sweden	58°29'00" N	10°56'00" E	20050101	20081231	20

data, root mean square value of the wave heights and average wave period, in equation 2.14 and deep water approximations the energy potential per year is calculated and shown in table 2.3.

Table 2.3: Average wave energy potential per meter of wave-front. x means that there was not enough valid data for that year.

Location	Energy [MWh/m per year]				
	2004	2005	2006	2007	2008
Iceland B.	510	460	480	550	580
Iceland H.	640	570	700	x	710
Ireland	x	750	660	650	890
Sweden	x	65	82	120	120

3 Wave energy converters

There are two cases of classification used for wave energy converters (WEC). The first classification is intended to describe the principle of operation and provide information on the geometry of the device. There are three groups in the first classification, *Point Absorber*, *Terminator*, and *Attenuator*. Point Absorbers are small devices relative to the wavelength of the incident waves. Attenuators and Terminators are wave energy converters which have finite dimensions relative to the incident wave field and one horizontal dimension that is dominant. Terminators are positioned with the dominant direction perpendicular to the incident waves while Attenuators are aligned with the incident wave direction [5]. The alternative classification is to label the converters as *First Generation*, *Second Generation*, or *Third Generation*. The first generation converters are onshore or near-shore. Second generation can be both offshore and near-shore and have physical dimensions that are much smaller than the wavelength of the waves from which the device is designed to extract energy. The third generation is defined as large-scale offshore device, both in terms of physical size and power output.

The device proposed by Daniel Ehrnberg [7] can be labelled as attenuator and third generation system. The device is described here below. Another wave energy converter that is also an attenuator and a third generation system is the Pelamis wave energy converter. The Pelamis is also described here below for comparison.

3.1 Description of Vigor wave energy converter

A new idea to harvest wave energy was proposed by Daniel Ehrnberg [7]. The device is called the Vigor Wave Energy Converter. In the thesis it will be referenced to as Vigor. This new device will use the motion of waves to build up pressure inside a hose that is on the surface of the ocean. The hose is filled with air in the crests of the waves and water at the troughs, as is shown in figure 3.1.

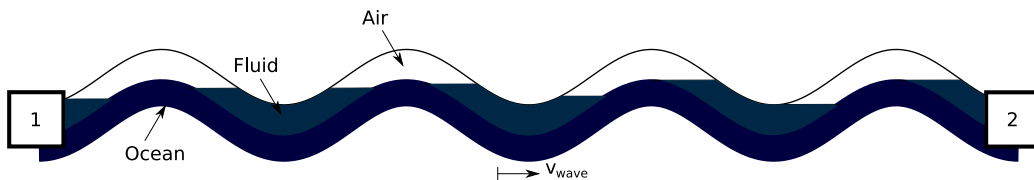


Figure 3.1: The Vigor wave energy converter. Notation 1 is the intake, 2 is the power take off system. The hose is filled with water at the troughs of the waves and air at the crests of the air. The scaling is not correct, the height of the wave is much smaller than the wave length.

The intake will periodically take in water and air. Properties of the waves, wave height and period will control the intake so that the right amount of air and water is in the hose. The water will be at the troughs of the waves while the air will be at the crests of the air. The water in the hose will therefore have the same velocity as the wave. The power take off system will let out the air under pressure, this will then result in that the water columns will move out of equilibrium. This forms a height difference in the water columns which can be seen as a pressure difference that can be utilised in a turbine to make mechanical energy. The mechanical energy can then be turned into electricity using a generator.

3.2 Other wave energy converter - Pelamis

There are large numbers of different wave energy converters in the design phase and trying to become commercial as previously mentioned. The WEC that has come the farthest is the Pelamis energy converter. The Pelamis consists of four slender semi-submerged cylinders. These cylinders are linked together with flexible joints. These flexible joints contain the power take off system. As the cylinders move up, down and to the sides, the pump, using hydraulic rams, high-pressure fluid through motors. The motors then drive electrical generators to produce electricity. The length of current production machines is 180 meters and the diameter is 4 meters. The machines have 4 power conversion modules, which are rated at 750 kW. The average energy potential of the Pelamis is between 1600 MWh/yr and 2600 MWh/yr, depending on site condition and wave resource [12].

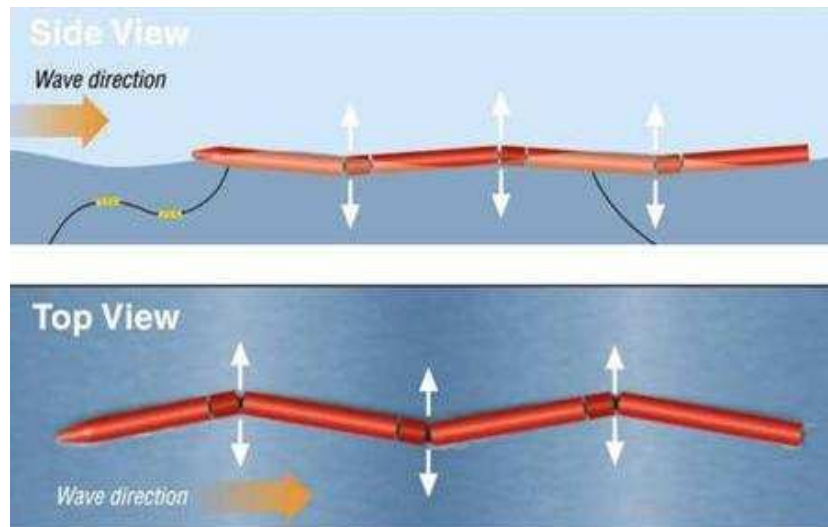


Figure 3.2: Movements of the Pelamis in the ocean [12]. The figure shows a earlier prototype that only has 3 power modulus.

4 Problem statements

As the Vigor wave energy converter is on the preliminary design states there are a number of problems still unsolved. Two problems are how the hose will behave in the ocean and how the power output is computed.

4.1 Interaction between the hose and the ocean

Having a large complex technical equipment in a harsh environment as the ocean is, represents a large number of problems, e.g. large strains and stresses on equipment in storms, movement of the equipment in complex wave interaction, and other environmental aspects. Here the focus will be on the basic problem of the interaction of a flexible hose with the ocean. Sections of the hose is filled with water while the remaining parts are filled with air. The interactions between the hose and the ocean are not fully understood. This influences the power output and is therefore of high importance and needs be understood, e.g. is the hose in the same phase as the waves and does it always lay on the surface of the ocean.

4.2 Flow inside the hose

To be able to calculate the power output from Vigor a large number of assumptions are needed. Some of the assumptions that have been used in past research e.g. [7] is that there is no pressure loss in the flow inside the hose. Here the pressure loss will be included in the power output calculations.

The problem is therefore to map the pressure losses of the flow within the hose. Pressure loss is a result of friction between the hose and the fluid. This is quite important as the power output is a function of the pressure potential in the hose.

5 Models description

To solve the the problems described in section 4 computer models are built and simulated to solve the problems. In this section the models, used to solve the problems, are described.

5.1 Interaction between the hose and the ocean

The interaction between the ocean and the hose can be modeled as a dynamic model with N degrees of freedom, where the forces act on the hose are found by applying Newton's second law. The system is described by N ordinary coupled differential equations of motion. Coupling occurs since the motions of each degree affects the other. The model can be described as a lump mass model as the continuous hose is cut into segments. Each segment is then described as a node with a mass and forces that act on the segment, that are added together [14]. The model is shown in figure 5.1.

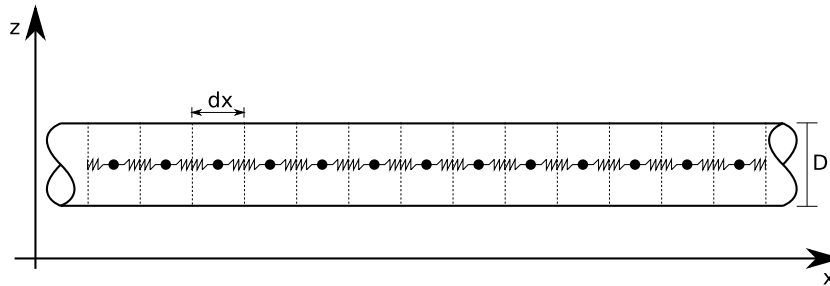


Figure 5.1: Hose cut into segments. dx is the length of each segment. D is the outer diameter of the hose.

The model takes only the vertical movement (z) and forces (F) into account because the vertical movement is of more concern in this stage. The horizontal forces are assumed to be zero and the nodes fixed so they do not move into the horizontal direction. This is assumed to be valid because the horizontal forces will be transferred to the mooring lines that anchor the device. The mass of each segment (dm_i) is either the hose mass (dm_{hose}) plus the air inside the hose (dm_{air}) or the hose mass plus water (dm_{water}) inside the hose segment.

The forces that act on each segment are due to gravitational acceleration F_g , buoyancy F_b , drag F_D , and longitudinal extension of the hose F_Y . The buoyancy force is due to the amount of the section that is submerged under water, that is volume of the segment that is submerged $dV_{submerged}$. The drag force is due to movement of the hose in the sea and the flow of the sea. The drag coefficient used is for a circular rod with flow around it, the coefficient is $C_D = 0.3$, and it is assumed that the flow is always turbulent [4]. The nodes are coupled together using the Hooke's law of elasticity, using Young's modulus, also called the elasticity modulus, of rubber Y for longitudinal extension of the hose. By using this law it implies that the elasticity of rubber can be assumed to be linear and the deflections are sufficiently small. This is a large assumption as the deflections can be rather high. Models that are non-linear, which can take into account the complex nature of rubber, have a high computational cost and would add hours to the computational time. Based on this high computational cost it is considered to be valid to use the simple model. The model is shown in figure 5.2. The rubber restrains against elongation with the force calculated by the Hooke's law. The force is transformed

into a vertical force that will increase as the nodes move further apart in the vertical direction. This implies that the hose equilibrium state is straight.

The single and double over-dots of coordinate represents the velocity and acceleration, respectively, of that coordinate (dz/dt and d^2z/dt^2).

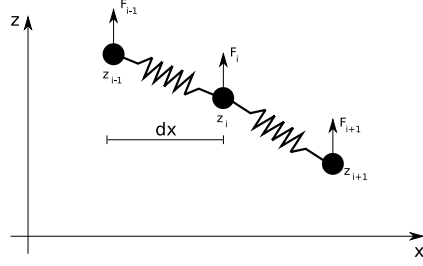


Figure 5.2: Hose cut into segments.

The forces on node i are then

$$\begin{aligned}
 F_{g,i} &= -dm_i g \\
 F_{b,i} &= dV_{\{\text{submerged}\}i} \rho_w g \\
 F_{D,i} &= -\frac{1}{2} \rho_w \dot{z}_i |\dot{z}_i| D_{out} dx C_D \\
 F_{Y,L,i} &= \frac{Y}{dx} \frac{\pi(D_{out}^2 - D_{in}^2)}{4} \left(\sqrt{dx^2 + (z_i - z_{i-1})^2} - dx \right) \\
 F_{Y,L,v,i} &= F_{Y,L,i} \frac{z_i - z_{i-1}}{\sqrt{dx^2 + (z_i - z_{i-1})^2}} \\
 F_{Y,R,i} &= \frac{Y}{dx} \frac{\pi(D_{out}^2 - D_{in}^2)}{4} \left(\sqrt{dx^2 + (z_{i+1} - z_i)^2} - dx \right) \\
 F_{Y,R,v,i} &= F_{Y,R,i} \frac{z_{i+1} - z_i}{\sqrt{dx^2 + (z_{i+1} - z_i)^2}}
 \end{aligned}$$

where

$$dm_i = \begin{cases} dm_{hose} + dm_{air} \\ dm_{hose} + dm_{water} \end{cases}$$

And where the density of the ocean is $\rho_w = 1030 \text{ kg/m}^3$, subscripts L and R is left and right respectively, and the subscript v means the vertical component of the force. The inside and the outside diameter of the hose is D_{in} and D_{out} respectively. The gravitational acceleration is $g = 9.82 \text{ m/s}^2$. Number of sections is from $i = [1, 2, \dots, L_{hose}/dx]$ The equation of motion for node i is then

$$dm_i \ddot{z}_i = F_i = F_{g,i} + F_{b,i} + F_{d,i} + F_{Y,R,v,i} - F_{Y,L,v,i} \quad (5.1)$$

The system of differential equations, shown in equation 5.1 is solved using the Runge-kutta method. The method finds the first solution using the initial conditions. The initial condition are that there are no waves and the hose is in equilibrium laying on the ocean. Waves are introduced after the first time step. Using the initial conditions the solutions for time step 1 is computed. The method then computes the time steps in sequence, using the previous solution. The method is used by implementing the function ode45 in MATLAB. For more information about the Runge-kutta method see e.g. [8].

5.2 Flow inside the hose

The power output depends on the pressure that is raised by the water columns. The pressure depends then on the amount the water columns are out of equilibrium and the pressure loss that happens due to the fluid flow. Therefore it is needed to find the pressure loss in the water columns. There are only few simple cases when it is possible to use theoretical solutions to calculate pressure losses, e.g. fully developed laminar flow in a circular pipe. The solutions available for more complicated cases therefore relies on experimental results and empirical relations rather than closed-form analytical solutions. Because of this the results from these methods are not “exact”. The results are estimates which show the magnitude of the factors and a norm of 10 percent error for the friction factors rather than exception [4]. This is the first step into finding the pressure losses before going into computational fluid dynamics (CFD), and even when using CFD there will be an error in the results as they to are also not based on analytical solutions [13]. One of the best ways to find solutions that do not have such large error margins, is to make experiments.

Having this in mind, the resulting solution to find the pressure loss, in a pipe, for all types of fully developed internal flows is

$$\Delta P_L = f \frac{L}{D_i} \frac{\rho V_{avg}^2}{2} \quad (5.2)$$

where f is the friction factor, L is the length of the pipe, D_i is the inside diameter of the pipe, ρ is the density of the fluid in the pipe, V_{avg} is the average velocity of the fluid.

The methods to find the friction factor are split into two cases. The first case is for laminar flow and the other is for turbulent flow. To find if the flow is laminar or turbulent flow the Reynolds number is used. The Reynolds number is defined as

$$Re = \left[\frac{\text{Inertial forces}}{\text{Viscous forces}} \right] = \frac{V_{avg} D}{\nu} = \frac{\rho V_{avg} D}{\mu} \quad (5.3)$$

where D is the characteristic length of the geometry, in this case it is the inside diameter of the pipe, $\nu = \rho/\mu$ is the kinematic viscosity of the fluid, ρ is the density of the fluid, and μ is the dynamic viscosity of the fluid. Laminar flow is defined as having Reynolds number smaller than $Re < 2300$ and turbulent flow is defined as having Reynolds number larger than $Re > 4000$. The region in between is defined as transition range, where the flow switches between laminar and turbulent flow. It is quite difficult to find solutions for that region and the solutions for turbulent flow will be used.

The friction factor for a fully developed laminar flow is

$$f = \frac{64\mu}{\rho D V_{avg}} \quad (5.4)$$

where μ is the dynamic viscosity of the fluid.

The friction factor for a fully developed turbulent flow cannot be found by theoretical analysis. The friction factor was therefore found by using experiments, for more discussion see e.g. [4]. In 1939, Cyril F. Colebrook combined the data from the experiments in the following implicit relation known as the Colebrook equation

$$\frac{1}{\sqrt{f}} = -2.0 \log_{10} \left(\frac{\epsilon/D}{3.7} + \frac{2.51}{Re\sqrt{f}} \right) \quad (5.5)$$

where ϵ is the roughness value of material and Re is the Reynolds number for the flow, found with equation 5.3. The equivalent roughness values for some common materials can be found in [4], the roughness value for rubber is given as $\epsilon = 0.01$ mm. It should be kept in mind that the values are for new pipes, and the relative roughness may increase with use as a result of corrosion, scale build-up, and precipitation. As a result, the friction factor may increase by a factor of 5 to 10 with use.

Although both equations 5.4 and 5.5 are developed for circular pipes they can be used for non-circular pipes by replacing the diameter by the hydraulic diameter

$$D_h = \frac{4A_c}{p} \quad (5.6)$$

where A_c is the cross sectional area and p is the wetted parameter.

To find the pressure loss for the flow inside the Vigor an energy equation for a steady, incompressible one-dimensional flow, on a unit-mass basis is used on the first water column in the hose. The energy is transferred, from the waves to the water inside, during the total length of the hose, so the largest height difference will be in the last column, $H_{wave} - D$. The model is shown in figure 5.3, and the energy equation is

$$\frac{P_1}{\rho} + \alpha_1 \frac{V_1^2}{2} + gz_1 = \frac{P_2}{\rho} + \alpha_2 \frac{V_2^2}{2} + gz_2 + \frac{\Delta P_L}{\rho} \quad (5.7)$$

where P is the pressure, z is the height of the surfaces of the water columns, V is

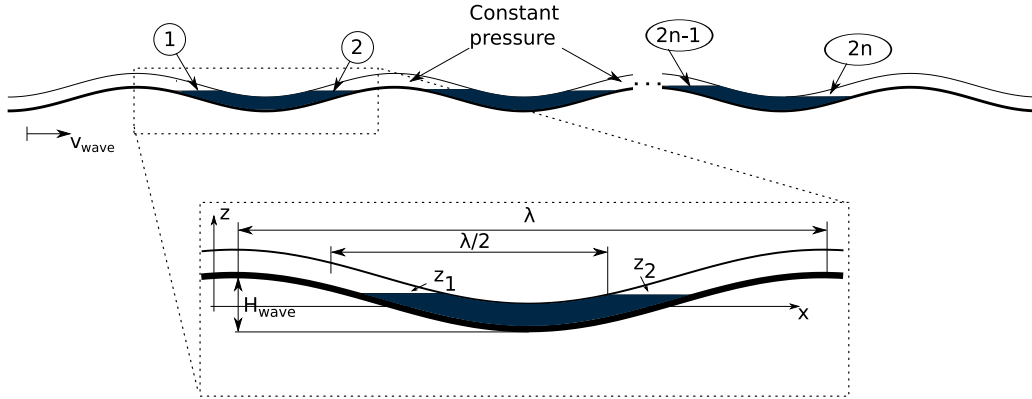


Figure 5.3: Water wave with hose filled with three water columns. Figure below shows wave and water columns characteristics.

the flow velocity, and α is the kinetic energy correction factors; $\alpha = 2$ for laminar flow, and $\alpha = 1.05$ for turbulent flow [4].

Because the velocities are the same, $V = V_1 = V_2$ at position 1 and 2, and it is assumed that the kinetic energy correction factors are the same at both positions, equation 5.7 simplifies

$$P_2 - P_1 = g\rho(z_1 - z_2) - \Delta P_L \quad (5.8)$$

Taking into account the rest of the water columns in the hose, the total pressure potential in the hose is

$$P_{2n} - P_1 = g\rho \left(\sum_i^{2n} z_{2i-1} - \sum_i^{2n} z_{2i} \right) - n\Delta P_L \quad (5.9)$$

where $n = L_{hose}/\lambda$ is the number of waves under the hose. It is also assumed that the pressure loss is the same for each water column.

This pressure difference can then be transformed into mechanical energy using a turbine. The energy output from the Vigor is, not taking into account losses in the turbine,

$$Power = VA_c(P_{2n} - P_1) \quad (5.10)$$

6 Results

The results from the models simulations of the interaction between the hose and the ocean as well as the flow inside the hose are shown and described in the following section. The interaction simulation is done for two types of hoses, each with different elasticity. The simulation for the flow inside the hose is used to optimize the potential power output. The simulation is run using wave data from four different locations in Iceland, Ireland and Sweden.

6.1 Interaction between the hose and the ocean

The results are based on a hose that has a circular cross section. The hose properties are based on the hose TUBO OREGON SUPER LIGHT from Mèrlett Technoplastic. This hose will be used for experiments in small scale prototype of the Vigor wave energy converter. The properties for the hose and the characteristics of the waves are shown in table 6.1. The young modulus for rubber is uncertain as it is different for each compound. Therefore a sensitive analysis is performed and the simulation done for two values, low Young modulus $Y_{low} = 0.1$ GPa, and high modulus $Y_{high} = 1$ GPa. Based on a monochromatic wave it is clear that the

Table 6.1: Properties for simulation

Property	Value	Description
D_o	0.15 m	Outside diameter
D_i	0.139 m	Inside diameter
ρ_{hose}	580 kg/m ³	Density
Y	[0.1 – 1] GPa	Young modulus for hose material
L_{hose}	200 m	Length of hose
T_{wave}	6 s	Wave period
H_{wave}	1 m	Wave height

interaction between the hose and the waves are as hoped for. This can be seen in figure 6.1. The hose follows the crest and the troughs very closely. For the hose with lower Young modulus it is clear that the hose is below at the troughs of the waves.

Figure 6.2 shows a close up of both the crest and the trough of the hose with the higher Young modulus. The hose lays on the surface on the crest but lays under the surface at the troughs.

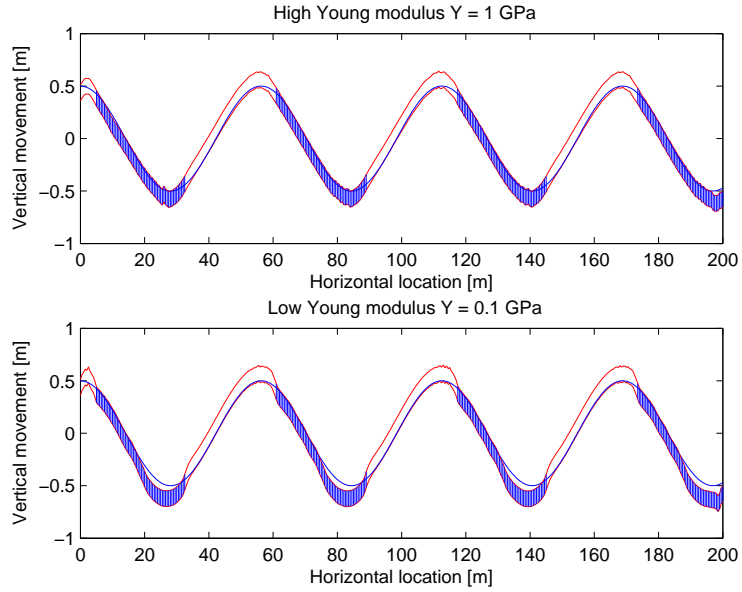


Figure 6.1: The interaction between the hose and the ocean with monochromatic waves. The figure above shows a model with high Young modulus and the model on the below figure has a low Young modulus. The red is the outlines of the hose, and the blue is water inside the hose. The waves are moving from left to right. The scaling is not correct.

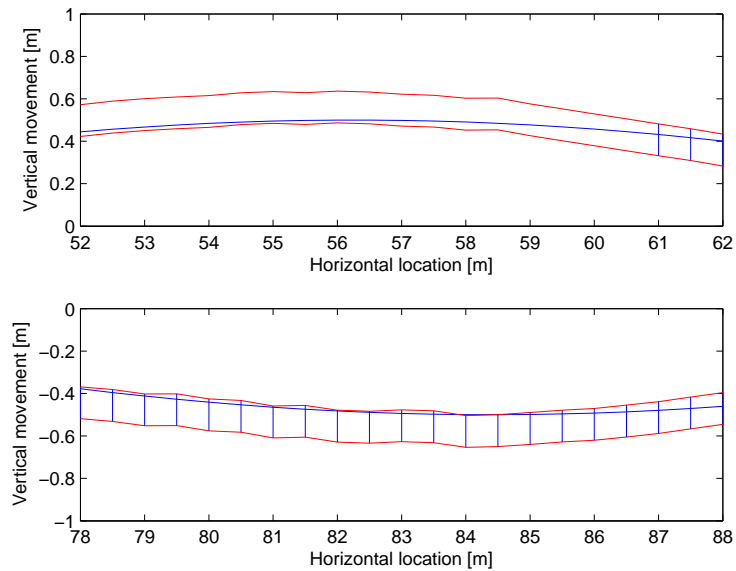


Figure 6.2: Close up of the crest, above, and the trough, below, of the hose for high Young modulus. The red is the outlines of the hose, and the blue vertical lines are water inside the hose. The blue horizontal lines are the ocean surface. The waves are moving from left to right. The scaling on the axis is not correct.

6.2 Flow inside the hose

The results presented here are based on the hose that has a length of $L_{hose} = 200$ meters. This is an arbitrary length which will be optimized in the future depending on the location. The roughness value used is for rubber and is $\epsilon = 0.01$ millimetres. A cross section of the hose is showed in figure 6.3 and these dimensions are varied to see how they influence the pressure potential in the unit and then the height dimension a is varied to find the optimal height which gives the best power potential.

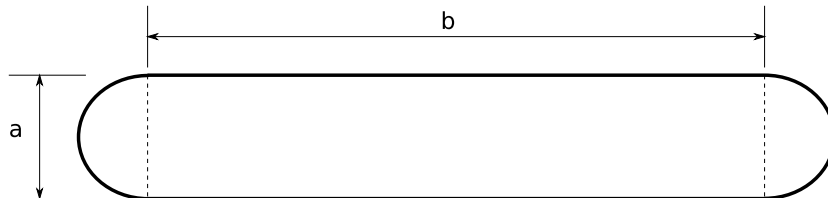


Figure 6.3: Cross section of the hose with dimensions.

Figure 6.4 shows how the dimension of the hose affects the potential pressure output. The different dimensions are shown in table 6.2. The curves show where the pressure potential is zero for the specific dimension of the hose. To the left of the lines the pressure is positive while to the right of the line the pressure is negative. The device produces energy when the pressure is positive. Figure 6.4 can be used to find if a specific hose works for a certain size of waves, in e.g. a wave tank that has monochromatic waves. A wave with the height of 5 meters and wave period of 5 seconds needs a hose with diameter larger than 0.2 meters.

Table 6.2: Dimensions of hose for figure 6.4.

Number	1	2	3	4	5	6	7	8	9	10	11	12
a [m]	0.1	0.2	0.4	0.6	0.8	1	0.5	1.0	1.5	2.0	2.5	3.0
b [m]	0	0	0	0	0	0	4	4	4	4	4	4

The power output is a function of the pressure potential in the hose and the flow rate through the hose, as can be seen in equation 5.10. The flow rate is a function of the cross sectional area of the hose. As the dimension a is increased the mass flow increases but the pressure potential decreases. Therefore there is some optimal a that will result in the largest power potential for the device depending on the wave resource. The optimum dimension is found by calculating the total energy output, using all of the data points in the wave data using different dimension a while the dimension b is constant, $b = 4$ meters. The result for the optimization is shown in figure 6.5 which show's that there is a optimum a in each location. The resulting optimum a is shown in table 6.3 for each location.

The potential power output, when the pressure loss is taken into account is shown in figure 6.6. The dimensions of the hose are, for a shown in table 6.3 for each location, $b = 4$ meters and length of $L_{hose} = 200$ meters. The potential power output is calculated using wave records from four different locations shown in table 2.2. Figure 6.6 shows that a large part of the waves are not producing energy. The curves show the potential power output in MW as function of wave period and height. The crosses are the wave data of each location.

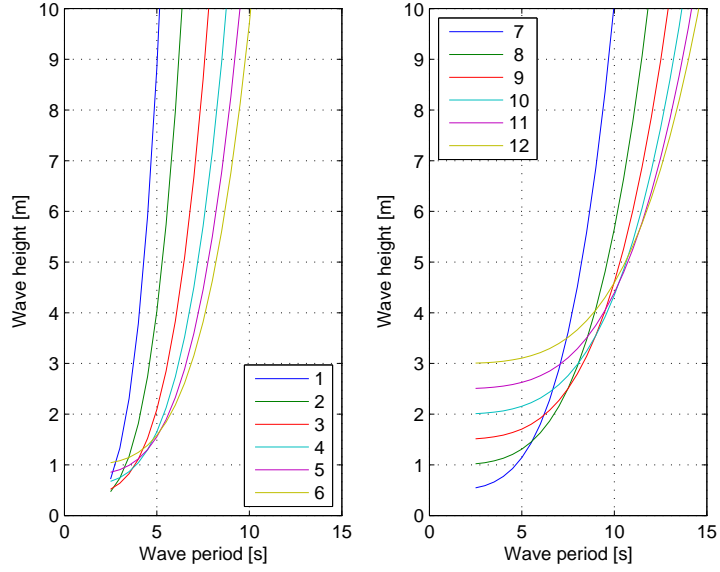


Figure 6.4: Curves show where the pressure is zero. There are 12 hoses with different diameters. The diameters are shown in table 6.2. The pressure is positive to the left of curves and negative to the right of curves.

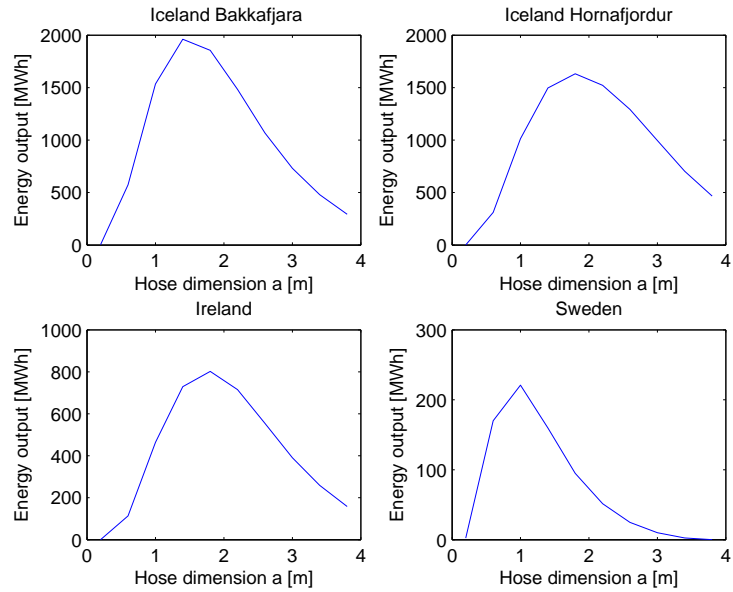


Figure 6.5: Curves show the energy output, calculated using wave data from each location, as a function of the dimension a .

Table 6.3: Optimal dimension a for the hose at each location.

Location	a [m]
Iceland B.	1.5
Iceland H.	1.8
Ireland	1.8
Sweden	1.0

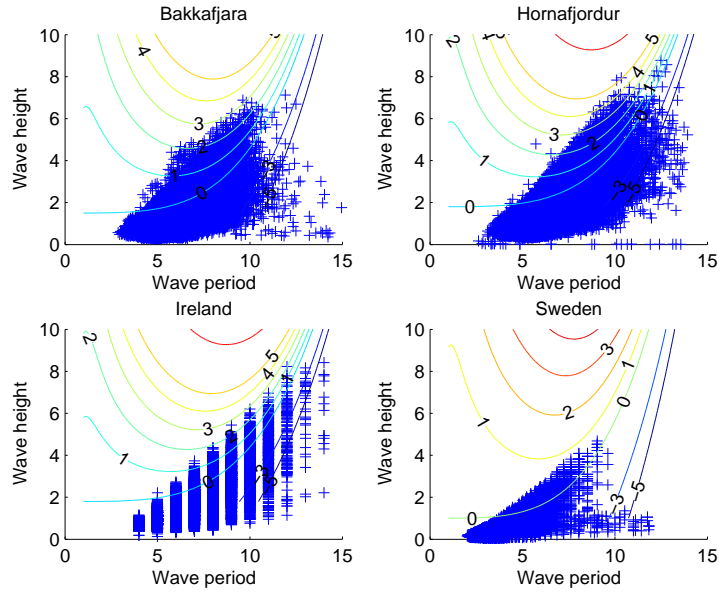


Figure 6.6: Curves show the potential power output in MW and the crosses represent the wave data. Wave data from Iceland Bakkafjara is in the upper-left corner, Iceland Hornafjordur in the upper-right corner, Ireland in lower-left corner and from Sweden in the lower-right corner.

The potential yearly energy output is shown in table 6.4. The average potential is the around, 400 MWh per year for Iceland Bakkafjara, also 400 MWh/yr for Iceland Hornafjordur, 200 MWh/yr for Ireland and 50 MWh/yr for Sweden. These values do not take into account the losses in the power take off system, i.e. losses in the turbine and the losses in the electricity generator. The potential wave energy

Table 6.4: Potential yearly energy output from Vigor. (x not enough data for the year)

Location	Energy [MWh/year]				
	2004	2005	2006	2007	2008
Iceland B.	390	320	360	420	490
Iceland H.	390	300	470	x	460
Ireland	x	200	120	130	360
Sweden	x	20	50	60	80

at each location, using the dimension in table 6.3, is shown in table 6.5.

As mentioned above, some of the waves are not producing energy through the Vigor converter. Table 6.6 shows how much of the time Vigor is producing energy. The maximum amount of the year is in Iceland and is 25% which means that it would have produced energy for around 2200 hours in the year 2008. The minimum is in Ireland, only 6% or around 500 hours that Vigor would have produced energy in 2007.

The early average efficiency of the Vigor is shown in table 6.7. The efficiency is calculated as the wave energy for the wave data compared to the potential energy produced by Vigor. The efficiency reaches nearly 60%, for some of the wave data.

Table 6.5: Average wave energy potential at each location. x means that there was not enough valid data for that year.

Location	Energy [MWh/year]				
	2004	2005	2006	2007	2008
Iceland B.	2800	2500	2600	3000	3200
Iceland H.	3700	3300	4000	x	4100
Ireland	x	4400	3800	3800	5200
Sweden	x	320	410	600	600

Table 6.6: Percent of the year when Vigor works (x means that that there was not enough valid data for the year).

Location	2004	2005	2006	2007	2008
Iceland B.	22%	17%	19%	24%	25%
Iceland H.	14%	11%	16%	x	14%
Ireland	x	11%	7%	6%	18%
Sweden	x	8%	11%	14%	16%

This high efficiency means that large part of the wave energy is transferred into useful mechanical energy.

Table 6.7: Average yearly efficiency of Vigor (x means that that there was not enough valid data for the year).

Location	2004	2005	2006	2007	2008
Iceland B.	24%	25%	24%	24%	25%
Iceland H.	22%	23%	24%	x	26%
Ireland	x	14%	15%	14%	16%
Sweden	x	21%	21%	21%	20%

6.2.1 Sensitive analysis

As mentioned in section 5 there are several uncertainties involved in some of the variables used in calculating pressure losses. To see how sensitive the results are for these uncertainties two variables are varied while other dimensions are constant. The length of the hose is $L_{hose} = 200$ meters, and the height is $a = 0.8$ meters and width is $b = 4$ meters. The variables that are varied are the roughness value, ϵ and the friction factor, f . The sensitiveness of the results are checked by seeing how the change in the variables will change the location of where the pressure, and the power, are zero. The results are shown in figure 6.7 and show that the model is more sensitive for change in the friction factor, as one might expect considering that the friction factor is a function of the roughness value, as can be seen in equation 5.5. Even though the value of the friction factor would be 15 percents lower the energy output would still be in the same range, hundreds MWh a year.

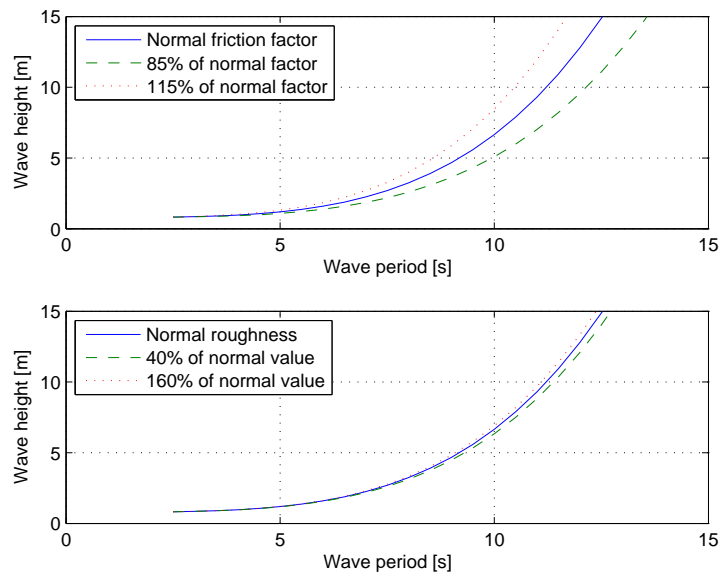


Figure 6.7: Sensitive analysis of the roughness value and the friction factor. Curves show when the pressure potential is zero. The pressure is positive to the left of curves and negative to the right of curves.

7 Conclusion

Wave energy converters have a large potential to be a part of the technology that generates electricity in the future. It is however still uncertain what approach will be used to transform the energy in waves into electricity. There is large number of approaches racing against each other to be the first one to reach commercial success. An attractive approach is the Vigor wave energy converter. The Vigor is still in the design phase and some initial design problems and initial solutions to the problems has been the focus of this thesis.

The problem of how the hose and the ocean ineract is complex. A simple model of the hose and the forces that act on the hose was constructed to solve the problem. This model was then simulated to see how the hose moves in the ocean. The result of the simulation indicates that the interaction is how it was assumed to be. The conclusion is that the hose moves in the same phase as the waves and lays on the surface of the ocean, in the troughs the hose is slightly submerged but on the crests the hose is on the surface of the ocean.

The model to calculate the power output of the Vigor wave energy converter was enhanced to take into account pressure losses. The pressure losses are a result of the friction between the fluid flow and the hose. The conclusion from using this enhanced model is that the pressure losses decrease the power potential of the Vigor quite substantially. The power output of the Vigor wave energy converter can reach up to 60% of the the theoretical maximum which is converting all of the wave energy into useful mechanical energy. The average efficiency is lower, around 20% of the conversion from wave energy into useful energy. The power potential of the Vigor energy converter depends on the wave resource and for the locations used in this thesis the largest potential is in Iceland and is 500 MWh in the year 2008.

7.1 Future research

There are still large numbers of assumptions related to both the model of the interaction between the hose and the ocean and to the pressure loss calculations. Further research is therefore needed to see if these assumptions are justified. For example assuming that rubber is linear elastic material is not valid because rubber is hyper-elastic material. Another aspect is the assumption that the pressure is constant in the air sections in the hose. This can be modeled in CFD to check if the assumption is valid.

Other parts that need to be researched are e.g. the energy transfer between the waves and the hose. Another problem is to see if the the pressure loss calculations are correct. An experiment should be done using similar material as is expected to be used in the commercial plant. A brief idea for the experiment is to measure the pressure loss in the hose using similar velocities as is expected to be in the hose during operation.

References

- [1] International Energy Agency. (2008). Key world energy statistics. *www.iea.org*. Accessed June 2009.
- [2] Energy Information Administration. (2009. May 27). International energy outlook 2009 - electricity [online]. *http://www.eia.doe.gov/oiaf/ieo/electricity.html*. Accessed 12 August 2009.
- [3] Cristian Azar. Sustainable energy futures course compendium, Autumn 2007. Chalmers University of Technology.
- [4] Yunus A. Çengel and John M. Cimbala. *Fluid Mechanics: Fundamentals and Applications*. McGraw-Hill, 2006.
- [5] João Cruz, editor. *Ocean wave energy: current status and future perspectives*. Springer, 2008.
- [6] Robert G. Dean and Robert A. Dalrymple. *Water Wave Mechanics for Engineers and Scientists*. World Scientific Publishing Co. Pte. Ltd., 1991.
- [7] Daniel Ehrnberg. A new wave energy principle and its working process. Master's thesis, Göteborg University, 2007.
- [8] J. Douglas Faires and Richard Burden. *Numerical Methods*. Brooks/Cole-Thomson Learning, 3rd edition, 2003.
- [9] Johannes Falnes. *Ocean Waves and Oscillating Systems*. Cambridge University Press, 2002.
- [10] Leo H. Holthuijsen. *Waves in Oceanic and Coastal Waters*. Cambridge, 2007.
- [11] B. Kinsman. *Wind Waves; Their Generation and Propagation on the Ocean Surface*. Courier Dover Publications, 2002.
- [12] Pelamis Wave Power Ltd. Pelamis wave power. *http://www.pelamiswave.com/*. Accessed June 2009.
- [13] H. K. Versteeg and W. Malalasekera. *An Introduction to Computational Fluid Dynamics; The Finite Volume Method*. Pearson Education Limited, 2nd edition, 2007.
- [14] James F. Wilson. *Dynamics of Offshore Structures*. John Wiley and Sons, 2nd edition, 2003.

Appendices

MATLAB programs

Interaction between the hose and the ocean

Movement of the hose

```

1 %
2 % Egill Maron Thorbergsson 090416
3 % Simulation of the movement of the hose in regular waves
4 % Modified 090609
5 % Both ends are large floating structures
6 %*****
7 function [y_hose x time r] = hose_movement(E)
8 % The program returns
9 % y_hose: [m m/s] the vertical position and velocity of the hose
10 % x: [m] the horizontal position of each segment
11 % time: [s] the time when the position and velocity were calculated
12 %*****
13
14 % Physical properties
15 rho.w = 1030; % [kg/m^3] Density of sea
16 rho.a = 1.3; % [kg/m^3] Density of air
17 g = 9.82; % [m/s^2] Acceleration due to gravity
18
19 % initial constants
20 delta.x = 0.5; % [m] Length of section
21 delta.t = 0.5; % [s] Time section
22 L.h = 200; % [m] length of hose - depends on specific location
23 % (optimized in the future)
24 x = 0:delta.x:L.h; % [m] Position of each segment
25 n.x = length(x); % [-] Number of nodes
26 t.start = 0; % [s] Time start
27 t.e = 30; % [s] Time length

```

```

28 | t_span = t.start:delta.t:t.e;      [%s] sections of time
29 |
30 | %   Hose properties
31 | rho.h = 580;                       [%kg/m^3] Density of the hose material
32 | %E   = 1e9;                         [%Pa] Young's modulus of the hose material (need to find)
33 | %n.h = 1;                           [%-] Number of hoses
34 | r.in  = 0.139/2;                   [%m] inner radius
35 | r.out = 0.15/2;                   [%m] Outer radius
36 | %L.h = 4*lambda;                   [%m] Length of hose
37 | width = 2*r.out;                  [%m] Total width of hose
38 | A.in  = pi*r.in^2;                 [%m^2] Inner area of hose
39 | A.mat = pi*(r.out^2 - r.in^2);     [%m^2] Area of the hoses material
40 | A.drag = width*delta.x;           [%m^2] Area for the drag force
41 | C.d   = 0.3;                      [%-] Drag coefficient
42 | k     = E * A.mat / delta.x;       [%N/m] Spring constant
43 | m.hose = A.mat * delta.x * rho.h;  [%kg] Mass of section of material ,
44 | m.air  = A.in * delta.x * rho.a;   [%kg] Mass of section of air
45 | m.water = A.in * delta.x * rho.w; [%kg] Mass of section of water
46 |
47 | %-----
48 | %   Finding the position of the hose so that it is in equilibrium with
49 | %   the sea
50 | %   [m] [Rectangle !] Where the hose(full with water is in equilibrium with the surface [F_g == F_lift]
51 | %y_eq_hose = r.out - (m.hose + m.water) / (2*r.out*delta.x * rho.w);
52 | %   [m] [Circle] Where the hose(full with water is in equilibrium with the surface [F_g == F_lift]
53 | y_eq_hose = r.out - 2 * (m.hose + m.water) / (pi*r.out*delta.x * rho.w);
54 | %-----
55 |
56 | %   Vertical force from end springs. The end nodes are free.
57 | F.ky(1) = 0;                       [%N] End spring
58 | F.ky(n.x+1) = 0;                   [%N] End spring
59 |
60 | %   End notes are modeled as boxes
61 | rho.ends = 700;                    [%kg/m^3] Density of end notes
62 | ends.H = 0.5;                      [%m] Height
63 | ends.area = 20;                    [%m^2] Bottom area
64 | ends.Vol = ends.area*ends.H;       [%m^3] volume of the ends
65 | F.submerged_end = ends.Vol*rho.w *g; [%N] Buoyancy forces
66 | C.d_end = 2.2;                     [%-] Drag coefficient Coefficient for square rod
67 | m.ends = ends.Vol*rho.ends;        [%kg] Mass of ends

```

```

68 F.g_ends      = - m.ends *g;      %[N] Gravity force for end notes
69
70 %          Calculate the maximum and minimum buoyancy force
71 %F.submerged  = 2 * r.out * width* delta.x * rho.w * g;  %[N] Force if fully submerged (for a rectangle)
72 F.submerged   = pi * r.out^2 * delta.x * rho.w * g;      %[N] Buoyancy Force if fully submerged (circle)
73 F.above       = 0;          %[N] Force if above water
74
75 %          [-] initial conditions for the hose
76 % [y_IC(:,1) y_IC(:,2)]      = wave(x,0);
77 % [y_IC dy_dt_IC]           = wave(x,0);
78 % y_initial_conditions(1:2:n.x*2) = y_IC;          %If the wave is not zero and the hose is floating
79 % y_initial_conditions(2:2:n.x*2) = dy_dt_IC;      %The hose has the same initial speed as the wave
80 %          [m] The wave starts at zero and we have the hose full of water and in equilibrium with the sea
81 y_initial_conditions(1:2:n.x*2) = y_eq_hose;
82 y_initial_conditions(2:2:n.x*2) = 0;      %[m/s] The hose has no initial speed
83 tic
84 %Solving the differential equations that describe the forces on the segments
85 [time y_hose] ...
86     = ode45( @(T,y) diff_eq_hose(T,y, A,n ,rho,F,g,k,m,r,delta,C,x,ends), t_span,y_initial_conditions);
87 toc
88
89 end%function
90 function dy_dt = diff_eq_hose(t,y, A,n ,rho,F,g,k,m,r,delta,C,x,ends)
91 % Differential equations that describe the forces that act on the segments
92 % of the hose.
93 % How dy_dt and y is set up
94 % dy_dt & y : (1,2) node 1 - (3,4) node 2 - ... - (2*n.x -1, 2*n.x) node n.x
95 %
96 dy_dt      = zeros(2*n.x,1);  %Preallocating memory for dy_dt
97 y_wave     = wave(t,x);      %[m] Computing position of the wave at time t for all x
98 y_wave_delayed = wave(t-1,x); %Delay for the position of the water inside the hose delayed
99
100 for i = 2:n.x %Need to compute this first because of F.ky(i+1)
101     %Force from rubber(as spring - Hook's law) between the nodes
102     %[N] Spring force (spring constant * deflection)
103     F.k(i) = k * ( sqrt( delta.x^2 + (y(2*i-1) - y(2*i-3))^2 ) - delta.x);
104     %[N] The vertical portion of the force
105     F.ky(i) = F.k(i) * ( y(2*i-1) - y(2*i-3) ) / sqrt(delta.x^2 + ( y(2*i-1) - y(2*i-3) )^2);
106 end%for
107

```



```

108 for i = 2:n.x-1
109     w = 0;%wave_vertical_velocity(t,x(i),y(2*i-1)); %[m/s] Vertical velocity for particles in ocean
110     %m.section = m.hose + m.water; %[kg] Mass of the node
111     %The mass of the section; air to the right of crest; water to the right of trough
112     m.section = m.hose + m.air*(y_wave_delayed(i)>0)+ m.water*(y_wave_delayed(i)<=0); %[kg]
113     F.g = - m.section *g; %[N] Gravity force
114     %[N] Linear approximation of the buoyancy force for a circle
115     F.lift = F.submerged / (2 * r.out) * (- y(2*i-1) + (y_wave(i) + r.out));
116     %[N] Find out if the hose is above or under water surface
117     F.lift = max( min(F.lift,F.submerged) ,F.above);
118     %[N] Drag force %need to check if it is under water
119     F.d = -0.5 * rho.w * (y(i*2)-w) * abs((y(i*2)-w))*A.drag*C.d;
120     if y(2*i-1) + r.out > y_wave(i) && sign(y(i*2)) == 1
121         %Check if upper part of the hose is above water level and if the hose
122         %is going upwards
123         F.d = 0; %Drag force for air - hose is above water
124     elseif y(2*i-1) - r.out > y_wave(i) && sign(y(i*2)) == -1
125         %Check if the lower part of the hose is above water level and if
126         %the hose is going down
127         F.d = 0; %Drag force for air - hose is above water
128     end
129     %Differential equations describing the forces on the nodes
130     dy_dt(2*i-1 , 1) = y(i*2); %[m/s] Speed
131     dy_dt(2*i , 1) = (1/m.section) * (F.g - F.ky(i) + F.ky(i+1) + F.d + F.lift); %[m/s^2] Acceleration
132 end%for
133
134 % [N] Gravity force
135 for i = [1, n.x]
136     %Compute the ends i=1 and i = n.x
137     w = 0;%vertical_velocity(t,x(i),y(2*i-1)); %[m/s] Vertical velocity for particles in ocean
138     %m.section = m.hose + m.water; %[kg] Mass of the node
139     %The mass of the section; air if crest; water if trough
140     %[N] buoyancy force for a square
141     F.lift = ends.area * (y_wave(i)-(y(2*i-1)-ends.H/2)) * rho.w * g;
142     %[N] Find out if the hose is above or under water surface
143     F.lift = max( min(F.lift,F.submerged_end) ,F.above);
144     %[N] Drag force %need to check if it is under water
145     F.d = -0.5 * rho.w * (y(i*2)-w) * abs((y(i*2)-w))*ends.area*C.d_end;
146     if y(2*i-1) + ends.H/2 > y_wave(i) && sign(y(i*2)) == 1
147         %Check if upper part of the hose is above water level and if the hose
148         %is going upwards

```

```
148     F.d      = 0;      %Drag force for air - hose is above water
149 elseif y(2*i-1) - ends.H/2 > y_wave(i) && sign(y(i*2)) == -1
150     %Check if the lower part of the hose is above water level and if
151     %the hose is going down
152     F.d      = 0;      %Drag force for air - hose is above water
153 end
154 %Differential equations describing the forces on the nodes
155 dy_dt(2*i-1 , 1)    = y(i*2); %[m/s] Speed
156 dy_dt(2*i    , 1)    = (1/m.ends) * (F.g_ends - F.ky(i) + F.ky(i+1) + F.d + F.lift); %[m/s^2] Acceleration
157 end
158 end%function
```

Waves

```
1 %
2 % Egill Maron Thorbergsson           090416
3 %
4 % Simulation of the surface position of waves
5 %
6 %*****
7 function z_wave = wave(t,x)
8 %[z_wave dz_wave_dt] = wave(x,t)
9 %
10 % Function for the wave calculations
11 % Assumption the t vector always starts at 0
12 % The wave starts at zero and is zero for the first t_zero seconds then it starts
13 % to increase linearly until at time t_start.
14 % z_wave(t,x):      time is in rows and x is in columns
15 %
16 %-----
17 % Exampel how to run the program
18 % time = [0:0.1:20];
19 % x = [0:0.1:60];
20 % y_wave = wave(time,x);
21 % %Plots an animation of the wave
22 % for i=1:length(time)
23 %     plot(x,y_wave(i,:))
24 %     axis([x(1) x(end) min(min(y_wave)) max(max(y_wave))])
25 %     pause(0.1)
26 % end
27 %-----
28
29 %Physical properties
30 g      = 9.82;           %[m/s^2]  Accelarition due to gravity
31 %Ocean wave properties
32 T      = 6;             %[s] period of waves
33 H      = 1;             %[m] height
34 h      = H/2;           %[m] amplitude
35 lambda = g*T^2/(2*pi);  %[m] wavelength [deep water wave]
36 sigma  = 2*pi/T;       %[rad/s] angular frequency
37 omega  = 2*pi/T;       %[rad/s] angular frequency
```

```

38 k      = 2*pi/lambda;      %[rad/m] wave number
39 %v.wave = lambda/T;        %[m/s] wave speed
40 t_zero  = 5;               %[s] How long is the wave zero
41 t_start = 15;              %[s] When the wave is full expanded
42 n.x     = length(x);       %[-] number of nodes
43 n.t     = length(t);       %[-] number of elements in time
44 z_wave  = zeros(n.t,n.x);  %[m] preallocating memory for z_wave and also initializing the vector
45 %Constants to make another wave that is different from the standard wave.
46 % const_wave_height = 1;
47 % const_wave_omega = 0.96;
48 % const_wave_lambda = 0.94;
49
50 for i = 1:n.t
51     %time is rows and x position is in columns
52     if t(i)<t_zero
53         z_wave(i,:) = h/100 * cos(-sigma * t(i) + k * x);
54     elseif t(i)>t_zero && t(i)<=t_start
55         %Check if time is in the between the linear space
56         %[m] Surface position of the ocean
57         z_wave(i,:) = h * cos(-sigma * t(i) + k * x) *(t(i)-t_zero)/(t_start-t_zero);
58         %Add another sin function to make more realistic wave
59         %z_wave(i,:) = (h * cos(-omega * t(i) + 2 * pi/lambda * x) + h/const_wave_height * ...
60         %cos(-omega/const_wave_omega*t(i) +2*pi/lambda/const_wave_lambda * x))*(t(i)-t_zero)/(t_start-t_zero);
61     elseif t(i)>t_start
62         %[m] Surface position of the ocean
63         z_wave(i,:) = h * cos(-sigma * t(i) + k * x);
64         %Add another sin function to make more realistic wave
65         %z_wave(i,:) = h * cos(-omega * t(i) + 2 * pi/lambda * x) + h/const_wave_height * ...
66         %cos(-omega/const_wave_omega*t(i) +2*pi/lambda/const_wave_lambda * x);
67     end%if
68 end%for

```

Flow inside the hose

Power output calculation

```
1 %
2 % Egill Maron Thorbergsson 090602
3 % Pressure and power calculations using one wave
4 %
5 %
6 %*****
7 function [p_height p_loss p_total Power] = pressure_power(T,H,r,width,epsilon,L_hose)
8 % Ouput
9 % p_height [Pa] Pressure for all water columns
10 % p_loss [Pa] Pressure loss for all water columns
11 % p_wc [Pa] Pressure at the outlet
12 % Input
13 % T [s] Wave period
14 % H [m] Wave height
15 % r [m] Hose radius
16 % width [m] Hose width between circle segments
17 % epsilon [m] Hose roughness
18 % L_hose [m] Hose length
19 %*****
20 %Physical properties
21 g = 9.82; %[m/s^2] Accelarition due to gravity
22 rho.w = 1030; %[kg/m^3] Density of sea
23 rho.air = 1.3; %[kg/m^3] Density of air
24 mu.w = 1.519e-3; %[kg/(m s)] Dynamic viscosity for liquid water at 5Â°C
25 lambda = g*T^2/(2*pi); %[m] wavelength [deep water wave]
26 v.wave = lambda/T; %[m/s] Wave speed
27 %sigma = 2*pi/T; %[rad/s] angular frequency
28 %k = 2*pi/lambda; %[rad/m] wave number
29 %n = L_hose/lambda; %[-] Number of water columns in the hose
30 n = 1; %[-] assumption about the pressure increase
31 L_wc = n*lambda/2; %[m] The total length of water column
32 A_c = pi * r.^2 + 2 * width .* r; %[m^2] cross-sectional area of the hose
33 peri = 2*pi .* r + 2 * width; %[m] wetted perimeter
34 D_h = 4*A_c/peri; %[m] Hydraulic diameter
35 vel_wat = sqrt(v.wave^2 + (v.wave/(lambda/2))^2); %[m/s] velocity of the water inside the hose
```

```

36 Vol_vel_wat = vel_wat * A_c;                               %[m^3/s] Volumetric flowrate
37 Re          = rho.w * vel_wat * D_h/mu.w;                 %[-] Reynolds number
38 f           = colebrook(epsilon,D_h,Re);                  %[-] Friction factor for turbulent flow
39 p_loss      = 0.5 * rho.w * f * vel_wat^2 * L.wc/D_h;     %[Pa] Pressure loss for all water columns
40 p_height    = n * rho.w * g * (H - 2 * r);                %[Pa] Pressure for all water columns
41 p_total     = p_height - p_loss;                           %[Pa] The total pressure at the end of hose
42 Power       = p_total * Vol_vel_wat;                       %[W] Total Power in the hose
43 end
44 function f = colebrook(epsilon,D,Re)
45 if Re < 2300                                             %Laminar flow
46     f = 64/Re;                                           %[-] friction factor for fully laminar flow in a circular pipe
47 elseif Re >= 2300                                       %Fully turbulent flow (2300 to 4000 is the transistion range)
48     f_sv = (-1.8*log10(6.9./Re + ((epsilon./D)./3.7).^1.11)).^(-2); %[-] Start value to find friction factor
49     f = fzero(@(f) findf(f,epsilon,D,Re) ,f_sv);         %[-] Friction factor for turbulent flow
50 end
51 end
52 function funct_value=findf(f,epsilon,D,Re)
53 %[-] Colebrook equation to find the friction factor
54 funct_value = -2 * log10((epsilon./D)./3.7 + 2.51./(Re.*sqrt(f)) ) - 1./sqrt(f);
55 end

```

Energy and efficiency of Vigor

```
1 % 090610
2 % Egill Maron Thorbergsson
3 % Program to find the power and energy from the vigor at a location using
4 % a wave data. The wave data is for one hour and is rms value of wave
5 % height and an average value of wave period.
6 %*****
7 clear all
8 i = 1; %[-] Chose what data is used see below
9 if i==1
10 [year H_rms T] = data_bakka; %[- m s] Data from Iceland Bakkafjara
11 r = 1.5/2;
12 elseif i==2
13 [year H_rms T] = data_horna; %[- m s] Data from Iceland Hornafjordur
14 r = 1.8/2;
15 elseif i==3
16 [year H_rms T] = data_ireland; %[- m s] Data from Ireland
17 r = 1.8/2;
18 elseif i == 4
19 [year H_rms T] = data_vaderoarna; %[- m s] Data from Sweden Vaderoarna
20 r = 0.5;
21 end
22
23 H_av = sqrt(pi/4)*H_rms; %[m] Use the average or most likely wave
24 H_av(isnan(H_av)) = 0; %[-] putting 0 instead of NAN so it is possible to calculate
25 T(isnan(T)) = 0; %[-] putting 0 instead of NAN so it is possible to calculate
26 n.H = length(H_av); %[-] Number of data points
27 n.T = length(T); %[-] Number of data points
28
29 L_hose = 200; %[m] Length of hose
30 width = 4; %[m] width between circle segments
31 r = 0.4; %[m] Radius of circle segments
32 epsilon = 0.01e-3; %[m] Roughness for the hose [rubber]
33 rho = 1025; %[kg/m^3] density of ocean
34 g = 9.82; %[m/s^2] gravity accelaration
35
36 points_year = []; %[-] Preallocating memory
37 E_year_vigor = []; %[-] Preallocating memory
```

```

38 E_year_wave = []; %[-] Preallocating memory
39 time_works = []; %[-] Preallocating memory
40 eff_year_av = []; %[-] Preallocating memory
41
42 E_total_wave = 3600*rho*g^2/16/pi*T.*H_rms.^2 * (width + r*2); %[J] Total energy in waves for one hour
43
44 for i = 1:n.H
45     if H_av(i) == 0 || T(i) == 0 %No data
46         p_height(i) = 0;
47         p_loss(i) = 0;
48         p_total(i) = 0;
49         Power(i) = 0;
50     else
51         %[Pa Pa Pa W] [Potential pressure; pressure loss; total pressure; Power output]
52         [p_height(i) p_loss(i) p_total(i) Power(i)] = pressure_power(T(i),H_av(i),r,width,epsilon,L_hose);
53     end
54 end
55
56 Power(Power<0) = 0; % [W] Put power to zero when power is negative, no power output
57 % Using another variable so it is possible to calculate total power from waves each year
58 E_total_wave_v = E_total_wave;
59 E_total_wave_v(Power<=0) = 0; %[-] Putting wave energy to zero is no output from vigor
60 for i = 2004:2008
61     points_year = [points_year nansum(year==i)]; %[-] number of data points in a year
62     time_works = [time_works sum(Power(year==i)>0)]; % [h] finds how many hours vigor works a year
63     % [J] finds the potential energy from waves for each year
64     E_year_wave = [E_year_wave nansum(E_total_wave(year==i))];
65     % [MWh] The Power output is only for a 1/2 of T because the hose is only filled to half with water
66     E_year_vigor = [E_year_vigor sum(Power(year==i))*0.5/1e6];
67     eff_year_av = [eff_year_av nanmean(Power(year==i)*0.5*3600./E_total_wave_v(year==i)')];
68 end
69 E_total_wave(Power<=0) = 0;
70 perc_year = time_works ./ points_year; %[-] Amount of the year that vigor works
71 % [J/J] efficiency for the vigor against waves waves when we have output
72 efficiency = Power*0.5*3600./E_total_wave_v';
73 eff_av = nanmean(efficiency); %[-] The average efficiency
74 plot(efficiency,'+') % Plot efficiency to see if it is on a reasonable region

```